Astrophysical radio background cannot explain the EDGES 21-cm signal: constraints from cooling of non-thermal electrons

Prateek Sharma[★]

Joint Astronomy Programme and Department of Physics, Indian Institute of Science, Bangalore 560012, India

ABSTRACT

Recently the EDGES experiment has claimed the detection of an absorption feature centred at 78 MHz. When interpreted as a signature of cosmic dawn, this feature appears at the correct wavelength (corresponding to a redshift range of $z \approx 15$–20) but is larger by at least a factor of two in amplitude compared to the standard 21-cm models. One way to explain the excess radio absorption is by the enhancement of the diffuse radio background at $\nu = 1.42$ GHz ($\lambda = 21$ cm) in the rest frame of the absorbing neutral hydrogen. Astrophysical scenarios, based on the acceleration of relativistic electrons by accretion on to supermassive black holes (SMBHs) and by supernovae (SN) from first stars, have been proposed to produce the enhanced radio background via synchrotron emission. In this letter, we show that either the synchrotron or the inverse-Compton (IC) cooling time for such electrons is at least three orders of magnitude shorter than the duration of the EDGES signal centred at $z \approx 17$, irrespective of the magnetic field strength. The synchrotron radio emission at 1.42 GHz due to rapidly cooling electrons is $\sim 10^3$ times smaller than the non-cooling estimate. Thus astrophysical scenarios for excess radio background proposed to explain the EDGES signal appear very unlikely.

Key words: radiation mechanisms: non-thermal – galaxies: high-redshift – intergalactic medium – dark ages, reionization, first stars – diffuse radiation.

1 INTRODUCTION

Very recently the EDGES (Experiment to Detect the Global Epoch of Reionization Signature) experiment has detected a broad ($\Delta \nu / \nu \approx 1/4$) absorption feature in the residual sky brightness temperature centred at $\nu \approx 78$ MHz (Bowman et al. 2018). Interpreting this dip in the brightness temperature as 21-cm absorption by the diffuse neutral intergalactic medium (IGM) at $z = 1.42$ GHz/78 MHz $- 1 \approx 17$ whose spin temperature is coupled to the gas temperature via the Wouthuysen–Field effect (Wouthuysen 1952; Field 1959; for a review see Pritchard & Loeb 2012), the absorption frequency range is consistent with the standard models for the reionization of the IGM. However, the amplitude of the absorption feature is at least a factor of two larger than predicted by such models.

The global brightness temperature corresponding to the emission/absorption of 21-cm photons for a background radiation characterized by a brightness temperature ($T_{bg} = T_R + T_{CMB}$; T_R and T_{CMB} are the brightness temperatures of a diffuse radio background and the CMB) at the redshift of absorption z is given by (equation 1

in Barkana 2018)

$$T_{21} = 36 x_{HI} \left(\frac{\Omega_b h}{0.0327} \right) \left(\frac{\Omega_m}{0.307} \right)^{-1/2} \left(\frac{1+z}{18} \right)^{1/2} \left(1 - \frac{T_{bg}}{T_S} \right) \tag{1}$$

in mK, where x_{HI} is the mass fraction of neutral hydrogen, Ω_b and Ω_m are the cosmic mean densities of baryons and matter, respectively, h is the Hubble parameter in units of 100 km s^{-1} Mpc^{-1}, and T_S is the spin temperature characterizing the level populations of the two hyperfine transition states. The spin temperature is expected to lie between the gas kinetic temperature (T_K) and the background radiation temperature (T_{bg}).

In the standard IGM evolution scenario all the background radiation at the relevant frequencies is due to the cosmic microwave background (CMB). The CMB temperature at the relevant redshift is

$$T_{CMB} \approx 49 \left(\frac{1+z}{18} \right) K \tag{2}$$

and the lowest possible gas kinetic temperature in the standard scenario is 7 K (as mentioned in Barkana 2018). Thus the minimum brightness temperature for the absorption trough at 78 MHz, according to equation (1), is -216 mK. The brightness temperature measured by EDGES is -500^{+200}_{-500} mK (errors correspond to 99 per cent [3σ] confidence intervals; Bowman et al. 2018). Thus, even the max-

★ E-mail: prateek@iisc.ac.in

imum value of the observationally inferred T_{21} (-300 mK) is lower than the minimum according to the standard scenario (-216 mK). From equation (1), the only way to lower T_{21} is to either raise T_{bg} (e.g. see Ewall-Wice et al. 2018; Fraser et al. 2018; Mirocha & Furlanetto 2018; Pospelov et al. 2018) or to lower T_S (Barkana et al. 2018; Berlin et al. 2018; Muñoz & Loeb 2018). In this letter, we investigate a subset of the former scenarios.

The presence of an additional radio background at 21 cm in the rest frame of the absorbing IGM (characterized by brightness temperature T_R) will increase the 21-cm absorption signal by an enhancement factor of

$$E = \frac{T_R/T_{CMB}}{1 - T_S/T_{CMB}} + 1 \approx \frac{T_R}{T_{CMB}} + 1, \tag{3}$$

since $T_S/T_{CMB} \approx T_K/T_{CMB} \sim 1/7 \ll 1$. Indeed there is an excess radio background measured at frequencies below 10 GHz, most recently highlighted by the ARCADE 2 experiment (Absolute Radiometer for Cosmology, Astrophysics and Diffuse Emission; Fixsen et al. 2011; see the recent conference summary on this by Singal et al. 2018). While this excess radio background cannot be accounted for by extragalactic radio point sources, most of it may be of Galactic origin (Subrahmanyan & Cowsik 2013). The brightness temperature of the excess radio background measured at 78 MHz is $\sim$600 K (see fig. 1 in Singal et al. 2018). We can explain the excess EDGES absorption if only a few K of this (comparable to the CMB brightness temperature at $z = 0$; see equation 3) is contributed by processes happening earlier than $z \sim 17$ (Feng & Holder 2018).

Astrophysical sources such as accreting supermassive black holes (SMBHs; Biermann et al. 2014; Ewall-Wice et al. 2018) and supernovae (SN) from the first stars (Mirocha & Furlanetto 2018) at $z \gtrsim 17$ can give the required excess radio background. This option, however, requires these sources to be $\sim$3 orders of magnitude more efficient radio emitters compared to their low-redshift counterparts.

In this letter, we show that the astrophysical mechanisms that require synchrotron emission from relativistic electrons to enhance the radio background at $z \approx 17$ are severely constrained because the cooling time (due to inverse-Compton and synchrotron losses) of these electrons is at least three orders of magnitude shorter than the duration of the EDGES absorption trough. This implies that the models that do not explicitly account for cooling of non-thermal electrons grossly overestimate the radio synchrotron background. Although the importance of inverse-Compton (IC) cooling at high redshifts and its contribution to the X-ray background is recognized (e.g. see Oh 2001; Ghisellini et al. 2014), here we focus on the cooling argument in the context of the recent EDGES result.

Unless stated otherwise, all quantities are expressed in physical units in the rest frame of the absorbing gas.

2 SYNCHROTRON RADIO BACKGROUND

In astrophysical scenarios, involving both SMBHs and SN, the excess radio background is produced by incoherent synchrotron emission due to relativistic electrons gyrating around magnetic field lines. In this letter, we do not model the radio emissivity due to accreting SMBHs and star formation at $z \sim 17$. In absence of observational constrains, the spectral/redshift variation of emission from these sources is highly uncertain. The radio emissivity models are based on extrapolations from low redshifts [e.g. see equations (4) and (5) in Ewall-Wice et al. 2018 (hereafter EW18); equation (5) in Mirocha & Furlanetto 2018 (hereafter MF18)]. Here we assume that these models for black hole accretion and star formation at $z \sim 17$, *which ignore cooling losses*, can be tuned to raise the ra-

dio background at 21 cm. In this letter, the radio source evolution is modelled by the source term S_γ in the one-zone model (equation 13), but we explicitly account for cooling losses which are very important at high redshifts. We show that the cooling of non-thermal electrons can suppress the radio background by $\sim 10^3$ relative to the non-cooling estimate.

The synchrotron emission at a frequency ν is related to the cyclotron frequency ($\nu_{cyc} = eB/2\pi m_e c$; e is the charge of an electron, B is magnetic field strength, m_e is electron mass, and c is the universal speed of light) by $\nu \sim \gamma^2 \nu_{cyc}$, where γ is the Lorentz factor of electrons with an isotropic momentum distribution. The Lorentz factor of electrons responsible for synchrotron emission at a frequency $\nu = 1.42$ GHz is given by

$$\gamma_{syn} \sim 730 \left(\frac{B}{10^{-3}G}\right)^{-1/2}. \tag{4}$$

The magnetic field strength in our equations refer to the regions in which electrons are confined to produce the excess radio background, and not to the strength of a global diffuse magnetic field. The synchrotron photons from a number of such sources are expected to result in an almost uniform large-scale radio background that may explain the global 21-cm absorption amplitude.

2.1 Synchrotron cooling time

The synchrotron cooling time $t_{syn} \sim \gamma m_e c^2/\gamma^2 u_B \sigma_T c$ ($u_B \equiv B^2/8\pi$ is magnetic energy density and σ_T is the Thomson scattering cross-section). Expressed in terms of B,

$$t_{syn} \sim 0.05 \text{Myr} \left(\frac{B}{10^{-3}G}\right)^{-3/2}. \tag{5}$$

3 INVERSE-COMPTON CONSIDERATIONS

Typically, the relativistic electrons producing synchrotron emission in radio also emit at much higher frequencies due to the Compton upscattering of the background radiation (in our case dominated by the CMB).

3.1 IC cooling time

The IC cooling time for relativistic electrons is $t_{IC} = \gamma m_e c^2/\gamma^2 u_{bg} \sigma_T c$ (u_{bg} is the energy density of the background photons). The ratio of the IC cooling time to the synchrotron cooling time *for the electrons producing the excess radio background* is

$$\frac{t_{IC}}{t_{syn}} \sim \frac{u_B}{u_{bg}} \sim 0.91 \left(\frac{B}{10^{-3}G}\right)^2 \left(\frac{1+z}{18}\right)^{-4}, \tag{6}$$

where we have assumed $u_{bg} = u_{CMB} = aT_{CMB}^4$ (a is the radiation constant). Thus the IC cooling time for these electrons (combining equation 6 with equation 5) is

$$t_{IC} \sim 0.046 \text{ Myr} \left(\frac{B}{10^{-3}G}\right)^{1/2} \left(\frac{1+z}{18}\right)^{-4}. \tag{7}$$

Fig. 1 shows the synchrotron and IC cooling time-scales as a function of the magnetic field strength at $z = 17$ and $z = 0$. Note that at $z = 0$, the IC and synchrotron cooling times cross at the field strength of $B \approx 3$ μG. The same crossover at $z = 17$ occurs at $B \sim 10^{-3}$ G. Also note that the maximum value of the cooling time ($t_{cool} \approx \min[t_{syn}, t_{IC}]$; see equation 14) at $z = 17$ is about four orders of magnitude shorter than at $z = 0$, implying that the cooling losses are much more important at higher redshifts than now.
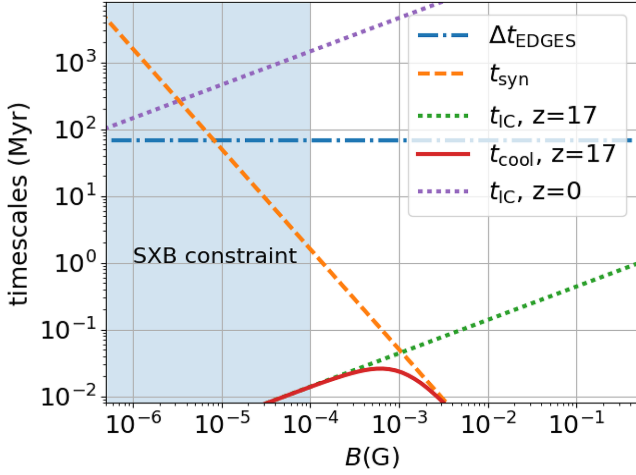
Figure 1. Important time-scales for the relativistic electrons producing the excess radio synchrotron background as a function of the magnetic field strength: the duration of the EDGES signal ($\Delta t_{\mathrm{EDGES}}$; equation 12), the synchrotron cooling time (t_{syn}; equation 5), the IC cooling time (t_{IC} at $z =$ 0, 17; equation 7), and the cooling time t_{cool} (equation 14) at $z = 17$. The relativistic electrons will cool at the shorter of the synchrotron and IC cooling time-scales, which at $z = 17$ is at least $\sim 10^3$ shorter than the duration of the EDGES absorption for all B. Magnetic field strength lower than $\sim 10^{-4}$ G (indicated by the blue-shaded region) is ruled out from the soft X-ray background constraint (see Section 3.2). An important time-scale, the electron replenishment time-scale in AGN/SN, is highly uncertain and not shown here but discussed in Section 4.1.

3.2 Soft X-ray background

Let us, for now, assume that synchrotron radio emission indeed produces the requisite radio background at $z \sim 17$. The same electrons are expected to upscatter the CMB photons and produce a uniform background at a frequency (see equation 4)

$$\nu_{\mathrm{IC}} \sim \gamma^2_{\mathrm{syn}} \nu_{\mathrm{bg}} \sim 1.5 \times 10^{18} \mathrm{Hz} \left(\frac{B}{10^{-3}\mathrm{G}} \right)^{-1} \left(\frac{1+z}{18} \right), \qquad (8)$$

which corresponds to 6.4 keV for the fiducial parameters. This IC background will be redshifted to soft X-rays (~ 0.36 keV, or equivalently, $\nu \sim 8 \times 10^{16}$ Hz) at $z = 0$.

The synchrotron emissivity of relativistic electrons is given by

$$\epsilon_{\nu,\mathrm{syn}} \sim \gamma^2_{\mathrm{syn}} u_B \sigma_T c \left[\frac{\mathrm{d}n}{\mathrm{d}\gamma} \frac{\mathrm{d}\gamma}{\mathrm{d}\nu} \right]_{\nu = \gamma^2_{\mathrm{syn}} \nu_{\mathrm{cyc}}}, \qquad (9)$$

where $\mathrm{d}n/\mathrm{d}\gamma \propto \gamma^{-p}$ is a power-law distribution of the relativistic electrons. The IC emissivity produced by the upscattering of the CMB *by the same electrons* is related to it by $\epsilon_{\nu,\mathrm{IC}}/\epsilon_{\nu,\mathrm{syn}} \sim u_{\mathrm{CMB}} \nu_{\mathrm{cyc}}/u_B \nu_{\mathrm{CMB}}$ (a consequence of $\nu_{\mathrm{syn/IC}} \sim \gamma^2 \nu_{\mathrm{cyc/CMB}}$). Therefore the ratio of IC and synchrotron emissivities per logarithmic interval in frequency is given by

$$\frac{(\nu \epsilon_\nu)_{\mathrm{IC}}}{(\nu \epsilon_\nu)_{\mathrm{syn}}} = \frac{u_{\mathrm{CMB}}}{u_B} \sim 1.1 \left(\frac{B}{10^{-3}\mathrm{G}} \right)^{-2} \left(\frac{1+z}{18} \right)^4. \qquad (10)$$

Now if this IC emission in X-rays travel to $z = 0$ without getting absorbed, for our fiducial B we expect a soft X-ray background (SXB) with νF_ν comparable to the radio background at $\nu \sim 78$ MHz measured at $z = 0$. Thus the spectral energy surface brightness density (νI_ν) at $\sim 8 \times 10^{16}$ Hz (0.36 keV) contributed by the synchrotron radio emitting electrons due to IC upscattering of the CMB is $\sim 3 \times 10^{-4}$ nW m^{-2} Sr^{-1}, a few per cent of the observed SXB (e.g. see fig. 2 in Singal et al. 2018 and compare the backgrounds

at 10^8 Hz and 10^{17} Hz). The constraint of not overproducing the SXB implies that $B \gtrsim 10^{-4}$ G in the sources is responsible for synchrotron radio emission (the blue-shaded region in Fig. 1 marks the field strengths ruled out by this constraint).

Moreover, such an SXB will have implications on the X-ray heating of the IGM, the evolution of the spin temperature, and the appearance of the 21-cm feature (see equation 1). We do not explore these issues in this letter (for a discussion, see EW18, MF18).

4 COOLING CONSTRAINT

The age of the Universe at the redshift of the EDGES absorption trough ($z \sim 17$), assuming a flat matter-only Universe (a good assumption at those redshifts), is

$$t_{\mathrm{age}} \sim 180 \, \mathrm{Myr} \left(\frac{1+z}{18} \right)^{-3/2}. \qquad (11)$$

The EDGES absorption trough is centred at $z \approx 17$ and has a duration $\Delta z/z \approx 1/4$. For a flat matter-only Universe $\Delta t/t = -3\Delta z/2(1+z)$, and therefore the time duration of the EDGES signal is

$$\Delta t_{\mathrm{EDGES}} = \frac{3}{2} t_{\mathrm{age}} \frac{\Delta z}{1+z} \approx 67.5 \, \mathrm{Myr} \left(\frac{1+z}{18} \right)^{-3/2} \frac{\Delta z/z}{1/4}. \qquad (12)$$

Now if an enhanced radio background has to explain the EDGES absorption amplitude, it must be present for at least the duration of $\Delta t_{\mathrm{EDGES}}$. If the relativistic electrons are accelerated only at the beginning of the absorption feature at $z \approx 20$ but are not replenished, they will cool off in $\lesssim 0.025$ Myr irrespective of B (see Fig. 1) and therefore the required radio background cannot be sustained for $\Delta t_{\mathrm{EDGES}}$. This implies that we need continuous injection of relativistic electrons to replenish cooling losses. But even with the continuous injection of electrons, cooling is expected to steepen the radio spectrum at the relevant frequencies, as we show next.

4.1 A one-zone model

The standard one-zone model for the evolution of $n_\gamma \equiv \mathrm{d}n/\mathrm{d}\gamma$ is given by (e.g. see equation (14) in Oh 2001; see also Sarazin 1999)

$$\frac{\partial n_\gamma}{\partial t} + \frac{\partial}{\partial \gamma}(\dot{\gamma} n_\gamma) = S_\gamma - \frac{n_\gamma}{t_{\mathrm{esc}}}, \qquad (13)$$

where $\dot{\gamma} = -\gamma/t_{\mathrm{cool}}$,

$$t_{\mathrm{cool}} = \frac{1}{t^{-1}_{\mathrm{syn}} + t^{-1}_{\mathrm{IC}}} \qquad (14)$$

is the cooling time due to synchrotron and IC cooling (we ignore adiabatic cooling), S_γ is the source term for relativistic electrons, and t_{esc} is the escape time-scale of relativistic electrons. The spectral index $\alpha_\nu \equiv \mathrm{d}\ln F_\nu/\mathrm{d}\ln \nu$ and the electron power-law index (p; $n_\gamma \propto \gamma^{-p}$) are related as $\alpha_\nu = -(p-1)/2$ (e.g. see Rybicki & Lightman 1986).

If there is no injection (i.e. $S_\gamma = 0$) but only cooling of an initial population of relativistic electrons, a cooling cut-off occurs at γ (the corresponding $\nu = \gamma^2 \nu_{\mathrm{cyc}}$) for which the cooling time equals the age of electrons; there are no electrons with a higher γ. The SED for this case is shown by the green dot–dashed line in Fig. 2.

Steady solution with injection and no cooling: In absence of cooling, the source term needed to produce an electron number density sufficient to produce the required radio background ($n_\gamma \propto \epsilon_{\nu,\mathrm{syn}}$; see equation 9) is given by $S_\gamma = n_\gamma/t_{\mathrm{esc}}$. Thus, in steady state the electron replenishment time equals the escape time (t_{esc}). Extrapolating from $z \sim 0$, EW18 and MF18 use a shallow spectral
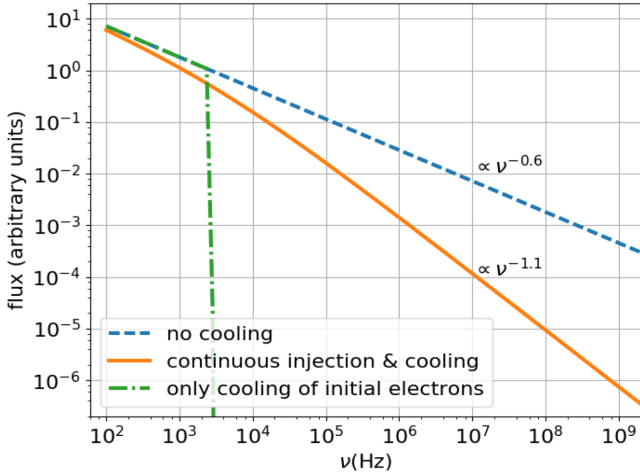
Figure 2. The average spectral energy distribution (SED) of the radio synchrotron sources at 18.25 Myr ($<\Delta t_{EDGES}$; corresponding to the cooling time of $\gamma = 1$ electrons) under different scenarios of electron cooling: (i) no cooling; (ii) continuous injection of electrons with cooling; and (iii) only cooling (and no continuous injection) of the initially relativistic electrons. For (ii), the spectral index ($d\ln F_\nu / d\ln \nu$) becomes steeper by 0.5 beyond the cooling break; for (iii), there is no emission at frequencies higher than the cooling cut-off. Since the minimum value of $\Delta t_{EDGES}/t_{cool} > 10^3$ for all field strengths (see Fig. 1), the cooling break at $\sim \Delta t_{EDGES}$ occurs at a very low frequency, and the flux at 1.42 GHz for (ii) is $\sim 10^3$ lower than (i).

index ($\alpha_\nu = -0.6, -0.7$ respectively) for the radio emission from their $z \approx 17$ sources. The corresponding electron indices are $p = 2.2$, 2.4, consistent with diffusive shock acceleration. These works do not account for cooling losses of the relativistic electrons, which are clearly very important at $z \sim 17$ as compared to $z \sim 0$ (see Fig. 1). Now we consider the effects of cooling.

Solution with injection and cooling: In presence of cooling, a cooling break appears for the solution of equation (13) at a γ for which the cooling time equals the age of electrons (t). For γs smaller than the cooling break $n_\gamma = S_\gamma t_{esc}$, the same as in the no-cooling case. However, for γs larger than the cooling break $\partial/\partial\gamma(\dot{\gamma} n_\gamma) \approx S_\gamma$. Since S_γ is assumed to be a power law (with $p = 2.2$) and $\dot{\gamma} \propto -\gamma^2$ (true for both synchrotron and IC losses), the slope of n_γ steepens by unity beyond the cooling break and the slope of the SED steepens by 0.5.

Fig. 2 shows the radio SEDs for models based on equation (13) (synchrotron emissivity and n_γ are related by equation 9) without injection (green dot–dashed line), with injection but no cooling (blue-dashed line), and with injection and cooling (orange-solid line). The dashed line shows the SED assumed by EW18 with a large enough S_γ ($S_\gamma \propto \gamma^{-2.2}$, equivalently $S_\nu \propto \nu^{-0.6}$), corresponding to their PopIII scenario (see their Fig. 1) that produces sufficient radio background. The solid line shows the SED with the same S_γ but affected by cooling (assuming $B = 10^{-3}$ G corresponding to the longest $t_{cool} \approx t_{syn}/2 \approx t_{IC}/2 \approx 0.025$ Myr; see Fig. 1) after a duration of $0.025 \times 730 \approx 18.25$ Myr ($< \Delta t_{EDGES} = 67.5$ Myr; equation 12), the time at which the cooling break for electrons reaches $\gamma = 1$ ($\nu = \nu_{cyc} \approx 2500$ Hz). [1]

The cooling time for non-relativistic electrons emitting cyclotron photons becomes independent of energy and the $t_{cool} \propto \gamma^{-1}$ scaling breaks down, but the SED at $\sim \Delta t_{EDGES}$ will definitely be below the

orange solid line in Fig. 2. Thus reading off the values at 1.42 GHz for the orange and blue lines in Fig. 2, we conclude that ignoring cooling losses overestimates the radio synchrotron flux by $\gtrsim 10^3$. Therefore, the source radio emissivities (equivalently S_γ) need to be boosted by $\sim 10^3$ to reproduce the EDGES absorption in presence of realistic cooling. This essentially rules out synchrotron radio background as a solution to the enhanced 21-cm absorption seen by EDGES because the models are already fine tuned to produce $\sim 10^3$ larger radio emission compared to $z \sim 0$ observations.

5 CONCLUSIONS

We conclude that astrophysical particle accelerators (first stars and supermassive black holes), with reasonable extrapolation from $z \sim 0$, cannot produce the radio synchrotron background at 1.42 GHz comparable to the CMB brightness temperature. Such a radio background is invoked by some models (e.g. EW18, MF18) to explain the excess 21-cm absorption signature claimed by the EDGES experiment. The principal difficulty is that the cooling time (shorter of the synchrotron and inverse-Compton cooling times) of the relevant relativistic electrons is at least three orders of magnitude shorter than the duration of the EDGES signal (see Fig. 1). To get the required radio background, various astrophysical scenarios have to enhance the radio emissivity by $\sim 10^3$ compared to the $z \sim 0$ models. In the presence of non-thermal cooling losses considered in this letter the required enhancement is expected to be $\gtrsim 10^6$, which seems almost impossible. Of course, there is the additional constraint from the soft X-ray background (see Section 3.2).

We note that the constraints in this letter do not apply to scenarios in which the excess radio background is not produced by relativistic electrons (e.g. Fraser et al. 2018; Pospelov et al. 2018). With stringent constraints on dark matter cooling (Barkana et al. 2018; Berlin et al. 2018; Muñoz & Loeb 2018) and on astrophysical models based on excess radio background, it is imperative that the EDGES signal be confirmed with other experiments. Thankfully there are several such ongoing experiments (e.g. Voytek et al. 2014; see Bernardi et al. 2016; Singh et al. 2017)

We end by noting that the arguments in this letter can be used to put tight constraints on the background radiation at high redshifts, independent of the fate of the EDGES signal.

REFERENCES

Barkana R., 2018, Nature, 555, 71
Barkana R., Outmezguine N. J., Redigolo D., Volansky T., 2018, preprint (arXiv:1803.03091)
Berlin A., Hooper D., Krnjaic G., McDermott S. D., 2018, *Phys. Rev. Lett.*, 121, 011102
Bernardi G. et al., 2016, MNRAS, 461, 2847
Biermann P. L., Nath B. B., Caramete L. I., Harms B. C., Stanev T., Becker Tjus J., 2014, MNRAS, 441, 1147
Bowman J. D., Rogers A. E. E., Monsalve R. A., Mozdzen T. J., Mahesh N., 2018, Nature, 555, 67

[1] Synchrotron self-absorption will become important at such low frequencies but the SED at 1.42 GHz (in the optically thin regime) will be unaffected.

Ewall-Wice A., Chang T.-C., Lazio J., Doré O., Seiffert M., Monsalve R. A., 2018, preprint (arXiv1803.01815) ((EW18)

Feng C., Holder G., 2018, *ApJ*, 858, L17

Field G. B., 1959, ApJ, 129, 536

Fixsen D. J. et al., 2011, ApJ, 734, 5

Fraser S. et al., 2018, preprint (arXiv:1803.03245)

Ghisellini G., Celotti A., Tavecchio F., Haardt F., 2014, MNRAS, 438, 2694

Mirocha J., Furlanetto S. R., 2018, preprint (arXiv:1803.03272) (MF18)

Muñoz J., Loeb A., 2018, Nature, 557, 684

Oh S. P., 2001, ApJ, 553, 499

Pospelov M., Pradler J., Ruderman J. T., Urbano A., 2018, Phys. Rev. Lett., 121, 031103

Pritchard J. R., Loeb A., 2012, Rep. Prog. Phys., 75, 086901

Rybicki G. B., Lightman A. P., 2004, Radiative Processes in Astrophysics , Wiley-VCH Verlag GmbH & Co. KGaA, Weinheim

Sarazin C. L., 1999, ApJ, 520, 529

Singal J. et al., 2018, PASP, 130, 036001

Singh S. et al., 2017, ApJ, 845, L12

Subrahmanyan R., Cowsik R., 2013, ApJ, 776, 42

Voytek T. C., Natarajan A., Jáuregui García J. M., Peterson J. B., López-Cruz O., 2014, ApJ, 782, L9

Wouthuysen S. A., 1952, AJ, 57, 31

This paper has been typeset from a TEX/LATEX file prepared by the author.